Raport Badawczy
Research Report

RB/14/2011

Exposure and intra-urban variation of emission-to-exposure relationship to different air pollutants in Warsaw, Poland

P. Holnicki, M. Tainio, Z. Nahorski

Instytut Badań Systemowych
Polska Akademia Nauk

Systems Research Institute
Polish Academy of Sciences

POLSKA AKADEMIA NAUK

Instytut Badań Systemowych

ul. Newelska 6

01-447 Warszawa

tel.: (+48) (22) 3810100

fax: (+48) (22) 3810105

Kierownik Zakładu zgłaszający pracę:
Prof. zw. dr hab. inż. Zbigniew Nahorski

Warszawa 2011

Exposure and intra-urban variation of emission-to-exposure relationship to different air pollutants in Warsaw, Poland

Piotr Holnicki [1], Marko Tainio [1,2*], Zbigniew Nahorski[1]

1. Systems Research Institute of the Polish Academy of Science, 01-447 Warsaw, Newelska 6, Poland.
2. National Institute for Health and Welfare (THL), P.O. Box 95, FI-70701 Kuopio, Finland.

* Corresponding author: Marko Tainio, e-mail: marko.tainio@ibspan.waw.pl, tel. +48-22-38-10-231, fax +48-22-38-10-105.

Abstract

Air pollution emissions in the urban area are causing significant adverse health effects. To effectively mitigate local adverse health effects, the sources of air pollution and their contribution to local air quality must be quantified. In this study, we estimate both exposure and emission-to-exposure relationships for several air pollutants and for four different emissions source categories in Warsaw, Poland. The emission-to-exposure relationship was illustrated by using the intake fraction (iF) concept. The exposure and iFs were predicted for primary particulate matter (PPM), nitrogen oxides (NOx), sulfur dioxide (SO2), Benso [a] Pyren (BaP), nickel (Ni), cadmium (Cd), and lead (Pb). The dispersion of pollutants was forecasted with CALPUFF dispersion model and by using the year 2005 meteorological data. The emission uncertainties were propagated through the dispersion model with the Monte Carlo techniques. The exposure and iFs were calculated by combining the population data with the predicted annual average air pollution concentrations. The population average exposure for fine particulate matter (PM2.5) was 7.1 $\mu g/m^3$ (95% confidence interval 6.6 -7.5 $\mu g/m^3$). 67% of this exposure was due to emissions from linear sources and 94% due to primary PM emissions, including resuspended PM. The predicted mean iFs varied from the 0.03 (NOx from point sources) to 47 (resuspended primary PM2.5 from linear sources) per million. The intra-urban variation of iF varied from 4.8 to 129 fold so that variation was highest for primary PM2.5 emitted from the other point sources and lowest for BaP and Cd emitted from the high point sources. These results show that, from the local emission sources, (i) traffic is contributing most of the exposure, and that (ii) the iF variation between sources and pollutants is substantial inside the urban area. The iF variation means that spatial emission mitigation actions would have different impact for local air quality.

Highlights

- We estimated exposure and emission-to-exposure relationships for several air pollutants in Warsaw, Poland, together with their estimated probability distributions due to emission inventory uncertainties;
- Intake fraction concept was used to describe the emission-to-exposure relationship;
- The highest intake fractions were predicted for the traffic emissions. This means that emission from traffic has higher potency to expose people than air pollution emissions from other sources;

Keywords (max 6)

Dispersion modeling; particulate matter; uncertainty analysis; intake fraction; exposure.

Abbreviations

BaP	Benzo [a] pyrene
CALPUFF	Steady-state meteorological and air quality modeling system
Cd	Cadmium
EEA	European Environment Agency
EU27	European Union 27 member states
HIA	Health Impact Assessment
IAM	Integrated Assessment Model
iF	Intake fraction
IMPACT	IMPact Assessment of Chemical Toxicants -model
Ni	Nickel
NOx	Nitrogen oxides
Pb	Lead
PITF	Population Inhalation Transfer Factor
PM	Particulate matter
PM10	Particulate matter with aerodynamic diameter less than 10 µm
PM2.5	Fine particulate matter with aerodynamic diameter less than 2.5 µm
PM_N	Nitrate (NO_3^-) aerosol (particulate matter)
PM_S	Sulfate ($SO_4^{=}$) aerosol (particulate matter)
PPM10	Primary PM10
PPM10_R	Primary PM10 caused by particle resuspension from the road surfacesPPM2.5 Primary PM2.5
PPM2.5_R	Primary PM2.5 caused by particle resuspension from the road surfaces
SO2	Sulfur dioxide

1. Introduction

Air quality forecasting models and integrated assessment models (IAM) are used to support air quality management decisions (e.g. http://gains.iiasa.ac.at/; ApSimon et al., 2002). These models are applied for the analysis of air pollution mitigation policies, for example, to indicate where the required air quality limits will be exceeded, and what emission mitigation strategy should be applied to reduce the adverse health effects caused by the air pollution.

The important part of IAM is to predict the dispersion of air pollution from the source to human breathing zone. The common way to incorporate this information to IAM is to use source-receptor matrices. The source-receptor matrix describes the change in the pollutant concentration (receptor) in relation to the unit variation of emission intensity (source). One of the modifications to traditional source receptor relationships is the intake fraction (iF) concept (Bennett, et al. 2002a). The iF is defined as an "*integrated incremental intake of a pollutant released from a source category and summed over all exposed individuals*" (Bennett, et al. 2002a). The iFs can be estimated for different pollutants and for different source categories (e.g. Bennett et al., 2002b, Tainio et al., 2009). For the air pollution, iFs are commonly predicted by combining the outdoor concentration data with the population density data.

Dispersion models and IAMs contain several uncertainties which might have impact also on resulting regulatory decisions. Previous studies have revealed (Russel and Dennis, 2000) that major uncertainties (measurement or estimation error) in dispersion models are due to the meteorological data and the emission inventory. Emission inventory for urban area usually encompasses various emission source categories, which are characterized by specific technological parameters, the composition of emitted compounds, emission intensity, and the range of uncertainty of emission data. The propagation of these emission uncertainties through the dispersion models is necessary to predict all the uncertainties in the IAM.

The variability is also an important factor, together with uncertainty, when planning mitigation actions. Previous studies have shown that the iF variation between emission source categories (e.g. Tainio et al., 2009; Taimisto et al., 2011) and intra-urban variation within the source categories (e.g. Greco et al., 2007) can be 10 to 100 fold. For example, Greco et al. (2007) find out that the iF variation for traffic related primary fine particulate matter (PM2.5) is from 0.8 to 53 per million for Boston, US. This result shows that not just the emission source category variation but also the intra-urban variation of emission-to-exposure relationship is important to be taken into account; especially for those source categories for which the location of emissions could be changed or the mitigation actions could be targeted to spatially smaller area.

In this study, we predict the contribution of local air pollution emissions for the air pollution concentrations in Warsaw, Poland. Main focus will be on estimation of (i) the impact of emission uncertainties for the predicted air pollution concentration, (ii) population exposure to air pollution in Warsaw, (iii) intake fractions (iF) for different air pollutants and for different emission source categories, and (iv) prediction of intra-urban variation of iF for different pollutant. From the different air pollutants, we will consider primary and secondary PM10 and PM2.5, Benzo [a] Pyren (BaP), nickel, cadmium, and lead.

2. Material and methods

The dispersion of air pollutants over the study area is predicted with the CALPUFF model (http://www.src.com/calpuff/calpuff1.htm). The emission uncertainties are propagated through the CALPUFF model by using Monte Carlo algorithms (Hanna et al., 1998, Moore and Londergan, 2001). After the dispersion modeling, the predicted air pollution concentration fields are combined with population data to calculate exposure and iFs for different air pollutants and source categories. Details of each phase are described in the following chapters.

2.1. Emission data

In the integrated assessment models, it is important to know what is the impact of the model uncertainty on model results. The emission inventory is one of the main sources uncertainty in the dispersion models. The emission uncertainty is especially important in the urban areas where emission field is usually characterized by spatial concentration of a number of emission sources. These differ in many parameters, such as: technological characteristics, emission intensity, composition of pollutants and also in range of emission uncertainty. For this reason, emission field for this study was split down into four categories:

- High point sources (represent energy sector, power and heating pants – relatively low uncertainty),
- Other point sources (industrial sources – medium uncertainty),
- Area sources (represent e.g. urban residential sector and some distributed industrial sources – high uncertainty),
- Linear sources (urban transportation system – high uncertainty).

The main pollutants considered in the sequel (primary and secondary) are shown in Table 1. The total emission field is composed of 16 high point sources (mainly heating plants), 1017 other industrial point sources, 877 area sources of the residential sector and 1156 linear sources of the urban transportation system. Location of point sources relates to their spatial coordinates. Area and linear sources are represented by 1km x 1km elements of spatial discretization of the domain.

The emission volumes and uncertainties for different pollutants are shown in Table 2. The emission uncertainty for each source category was individually generated for each pollutant by assuming normal distribution. To avoid creating technologically unrealistic sets of emission data (Page et al., 2003; Holnicki et al., 2010), the Monte Carlo sampling took into account correlations between key compounds for each source category.

2.2. Forecasting of air pollution concentrations

CALPUFF model computations were performed for 2005 emission and meteorological datasets, with 1 hr time interval of the input data. Annual mean concentrations of different air pollutants were predicted for 563 receptor points located at 1 km x 1 km grid discretization nodes over the Warsaw (Figure 1). Monte Carlo technique was used to propagate emission uncertainty through the dispersion model. Simulations were performed for 2000 randomly generated sets of input emission data and then utilized by atmospheric transport model CALPUFF. The results of CALPUFF calculations were recorded in a database (Holnicki et al., 2010) that contain information from annual average

concentrations and standard deviation of each pollutants emitting from four source categories for each 563 receptor point. This information was later used to calculate the exposure and iFs (see description below).

2.3. Validation of the dispersion model

Dispersion model performance was validated by comparing predicted air pollution concentrations with the observations. Figure 2 presents comparison of predicted averaged concentration of particulate matter (PM10) with measurement values registered at monitoring stations. Locations of monitoring stations are shown in Figure 1. The dashed lines show ranges of the factor of 2, usually adopted in comparison of modeling and observed atmospheric pollution data. The predicted PM10 concentrations were following the measured concentrations. Contribution of the inflow of PM10 from emission sources located outside computational domain was included in this comparison as an average regional PM10 concentration.

2.4. Estimation of population average exposure

The exposure of Warsaw population to different air pollutants was estimated by comparing the population data with the forecasted air pollution concentrations. Population data was obtained from the European Environment Agency (EEA) (EEA, 2009). The spatial resolution of EEA population data is 100 m x 100 m and it covers all EU27 countries. The population of study area was estimated from the EEA population data by taking 1 km buffers around each 563 receptor points and then calculating the population around each receptor point. Each 100 m x 100 m population grid was joined only for one receptor point to avoid double counting. The population of Warsaw over all the receptor points was 1 790 872. These calculations were done with the ESRI ArcMap version 9.3.

Average concentrations of air pollutants were estimated by calculating the average air pollution concentrations over the 563 receptor points. Exposure was calculated by assuming that outdoor concentration of air pollutants represents the population exposure. The exposure was estimated by calculating the population weighted air pollution concentration with following equation:

$$E = \sum_i \frac{C_i Pop_i}{Pop} \quad (1)$$

In this equation, E is the exposure for air pollution (unit: µg/m3 or ng/m3), C_i is forecasted air pollution concentration (unit: µg/m^3 or ng/m3) in the receptor point i, Pop_i is the number of population in the receptor point i. Both average concentration and exposure were calculated for each pollutants and for each emission source category.

The forecasted annual average air pollution concentrations and standard deviations for the forecasts were downloaded from the dedicated database to the Monte Carlo simulation program Analytica version 4.3 (http://www.lumina.com/). The concentration uncertainties were propagated through

196 the model with 1000 iterations. Correlations were taken into account so that for the same pollutant
197 emitted from the same sources, the iterations for different receptor points had approximately 90%
198 correlation. Thus, we assume that forecasted concentrations e.g. for primary PM2.5 due to linear
199 sources correlate between different receptors.

200 **2.5. Intake fraction (iF)**

201 The iF was calculated with the equation:

202

203 $$iF = \sum_i \frac{C_i Pop_i BR}{Q} \quad (2)$$

204

205 where iF is the intake fraction; C_i is the predicted concentration increase of air pollutant in a
206 receptor point i (g/m^3); Pop_i is the population number in receptor point i; BR is the average
207 breathing rate; and Q is the emission strength (g/s). A breathing rate of $20 m^3$/day/person was used
208 in all the calculations.

209 The iFs were estimated separately for four different emissions source categories and for different air
210 pollutants. For SO2 and NOx the emissions were multiplied with the factors 0.67 and 0.48,
211 respectively, to take into account the differences in chemical composition of inhaled PM versus
212 emitted PM (see Table 1). Thus, the iF takes into account that molecular weight will increase due to
213 chemical reactions in the atmosphere.

214 **3. Results**

215 **3.1. Air pollution concentrations and exposure**

216 The average concentrations and exposure for different air pollutants are presented in Figure 3. From
217 the four modeled emissions source categories, linear and area sources were contributing most to
218 the predicted air pollution concentrations. Only for PM_S the high point sources emission category
219 was more significant emission source than linear or area sources.

220 Average exposure to PM2.5 air pollution was 7.1 $\mu g/m^3$ (95% confidence interval 6.6-7.5). From this
221 exposure, 94 % was due to PPM2.5 emissions and 67% due primary PM2.5 and precursor gas
222 emissions from the linear sources. The contribution of secondary aerosols and point sources for the
223 average PM2.5 exposure was 6% and 8%, respectively. The results indicates that, from local sources,
224 the PPM2.5 emission from traffic is the most prominent target for emission mitigation actions while
225 high point sources has only minor impact for local air quality.

226 For BaP, Cd, Ni and Pb the linear sources were contributing 56% to 100% of total exposure. Point
227 sources were having only minor impact to exposure also for these pollutants.

228 For almost all the pollutants and source categories, the exposure, calculated as a population
229 weighted outdoor concentrations, was higher than average concentrations of the same pollutants
230 (Figure 3). For the primary PM and Pb emitted from the linear sources, the exposure was
231 approximately 65% higher than average concentration. For the BaP, Cd and Ni the opposite was true
232 so that exposure levels were 11% lower than average concentrations. For the area sources, exposure

was 1% to 6% higher than average concentration for all the pollutants. These results show that, on the average, population and emissions are correlated in the study area but that there are also exception for this rule.

The emission uncertainties were contributing only little to the uncertainty of the average concentration estimates (Figure 3) while for the individual receptor point the impact was greater. For example, Figure 4 illustrates the PM10, PM-S and PM-N concentrations, contributions of different source categories and resulting concentration uncertainties for receptor No. 275. All predicted concentration estimates are much more uncertain than the average concentrations for these same pollutants in study area (comparison of Figures 3 and 4). This is due to location of this receptor in the area of intensive car traffic and substantial contribution of very uncertain linear sources in the resulting concentration, especially for PM10 and PM-N. On the other hand, relatively low uncertainty for PM_S follows from substantial contribution of more certain point sources (compare Table 2 and Figure 4).

3.2. Intake fractions

The intake fractions (iF) for different source categories and air pollutants are presented in Table 3. The highest iF was observed for the PPM10 and PPM2.5 emissions from linear sources. After linear sources, the highest iFs were predicted for the area sources followed by other point sources and high point sources. The difference in average iF between linear sources and high point sources was 50 fold for PPM2.5. This means that, per emission volume, the PPM2.5 emission from linear sources is 50 times more harmful than similar emission from the high point sources, if same exposure-response function is assume for both PMs. However, this calculation took into account only local population and result would be different if the dispersion outside the Warsaw was taken into account.

For BaP, Cd and Ni the iFs were highest for the area sources and second highest for the linear sources.

The intra-urban variation of iF was large (Table 3). For PPM2.5, the lowest iF predicted for one emission source was 0.05 per million and highest 100 per million. The difference between smallest and highest predicted iF for PPM2.5 emitted from other point sources was approximately 120 fold showing great differences in exposure potential between individual sources (Figure 5).

4. Discussion

We have examined the concentration of different air pollutants and the exposure of local population for these air pollutants in Warsaw, Poland. From the four modeled source categories, the emissions from linear sources were causing most of the exposure for most of the pollutants. The importance of the linear sources over the other sources is mainly due to high correlation of emission location with population location, and low emission height. This can be observed from our results by comparing the iF estimates for linear sources with iF estimates for other source categories (Table 3). However, for some air pollutants, especially for Cd, Ni and Pb, the area sources had higher iF than linear sources. Even for these pollutants, the linear sources were contributing more to the exposure, in

comparison to area sources, due to higher emission volumes (Table 2). All these results highlight the importance of the traffic to the local air quality, exposure and population health.

The substantial emission uncertainties were contributing only small amount of uncertainty for the predicted air pollution concentrations. For example, for the receptor 275 the PPM10 concentration uncertainty was ±18 but for the average PPM10 concentration over the study area, the uncertainty was ± 6%. This uncertainty is much lower than the ± 40% emission uncertainty that was assumed for the PPM10 emission for the linear and area sources (Table 2).

The ± 6% concentration uncertainty is small in comparison to other uncertainties in the IAMs. For example, the Wang et al. (2006) predicted iFs for four different source categories in China. As a part of the study they performed a set of sensitivity analyses. Highest uncertainties were related to the size of the modeling domain (+200-300% impact for mean iF estimates), population resolution (-49%, +95%) and to half-life of SO2 (+55%) (Table 5, Wang et al., 2006). These uncertainties are not necessary relevant for the present study but they illustrate the range of uncertainties commonly found in IAM studies. When the health effect estimation is included in IAM, the uncertainties can be even larger. For example, in Tainio et al. (2010) study the mean predicted premature mortality due to primary PM2.5 emission from Finland was 209 deaths per year and uncertainty range from 6 to 739 deaths per year. This corresponds -97%, +350% uncertainty around the mean estimate.

The intra-urban variation of iF was much larger than the impact of the emission inventory uncertainty (Table 3, Figure 5). The difference between smallest and highest predicted iF varied between 5 to 130 fold for different pollutants and sources. The variation was highest for the PM air pollution emitted from other point sources and smallest for Cd and BaP emitted from the high point sources. In general, the iF variation was highest for the linear sources and area sources.

The intra-urban variation of iF for different pollutants are similar to the iFs estimated in previous studies. For example, Greco et al. (2007 estimated iFs separately for 23 398 road segments inside the Boston, US, and the dispersion of primary PM2.5 was calculated within 5000 m from the road segments. The iF variation between segments was 0.8 to 53 per million while the mean was 12 per million. In present study, the respective values for linear sources were 1.5, 100 and 38 per million. Together these studies show that the iF variation inside the urban area is significant and this will have impact for emission mitigation actions that are targeting only part of the city (e.g. congestion).

Also for the area sources the iF variation predicted in present study is similar to iF variation predicted in previous studies. In Vancouver, Canada, the iF values for wood burning were estimated to be 13 per million (geometric mean) and uncertainty range 6.6 to 24 per million (one geometric standard deviation) (Ries et al., 2009). In Ries et al. (2000), the iFs were based on measured concentration and a land use regression model designed to estimate spatial variation of wood burn related primary PM2.5 in the study area. In Lai et al. (2000) a cumulative population inhalation transfer factor's (PITF) for the hypothetical urban area was calculated. For outdoor sources they estimated PITF values between 4.4. and 44 per million, depending on the wind speed. The definition of PITF is identical with iF so that the units are comparable. Both of these estimates are similar to mean and variation of If for PPM2.5 due to area sources predicted in present study (Table 3).

For high point sources, Wang et al. (2006) estimated iFs for 49 different power plants from six different urban areas in China. The average iF for TSP was 3.0 per million and variation from 0.41 to

17.9. The representative values for high point sources from the present study were 0.81, 0.050 and 3.1 per million, respectively. Thus, our iFs are approximately in order of magnitude lower than the iFs estimated in Wang et al. (2006) study. The Wang et al. study took into account exposure within 50 km from the sources so the one magnitude differences might be due to larger study domain and larger population density.

The literature search in the Intake Fraction Database (http://www.ktl.fi/expoplatform/) and in the ISI Web of Knowledge (http://apps.webofknowledge.com/) revealed only limited amount of iF studies for other air pollutants than PM. For metals, Spadaro and Rabl (2004) used a multimedia pathway model to estimate exposure and iFs for metals in average European setting. For the Cd, Ni and Pb they estimated iFs equal to 3.9, 3.9 and 7.1 per million, respectively. In present study, the average iF for these same metals were 5.9, 5.9 and 40 per million, respectively. Although Spadaro and Rabl (2004) study was based on average central-European condition and present study to urban condition, the iF estimates are close to each other for Cd and Ni. For Pb the difference is substantial and probably due to high portion of Pb emissions emitted from the linear sources.

For BaP, previous studies have used different methods to estimate the iF through different exposure routes. Humbert et al. (2009) estimated iF for BaP, and a number of other pollutants, using multimedia, multi-pathway model IMPACT North America (version 1.0). The iF for BaP for urban setting was 5.0 per million. Maximum estimated iF for urban setting was 30 per million. In the present study the average iF for BaP was 6.0 per million. The other study from North America assumed average iF for BaP to be 24 per million (Bennett et al., 2002b). However, the later iF was for air release taking into account exposure through the ingestion. This suggests that the iF for BaP could potentially be higher if also other exposure routs beside the inhalation would be taken into account.

4.1. Uncertainties

The main non-quantified uncertainties were recognized to be the amount of population, lack of population location data and indoor-outdoor penetration of pollutants. Also, the influence of variations in year weather conditions was not considered.

In the present study, the population of Warsaw was assumed to be 1.7 million. This estimate is also close to official population count, generated by the city of Warsaw. However, the Warsaw has large non-official populations that live in the city but are registered in other parts of the country. Unofficial estimates have assumed that real population might be 3 million, or even more. If the true population of Warsaw is significantly higher, it means that the iFs calculated in the present study underestimate the true exposure by underestimating the amount of people in study area. Also, non-official population might live in different areas of the city than official one, which would result in changes both in iFs and exposure estimates. Unfortunately, the importance of this uncertainty is impossible to quantify with the current amount data.

The other main uncertainty relates to assumption of population location. We assumed that the outdoor concentrations of pollutants in people's home address represent their exposure. This bias the exposure estimates both upward and downward. The infiltration of pollutants from outdoor to indoor is reducing the exposure for outdoor originated pollutants because only some of the pollutants penetrate indoor. This bias our iF estimates upward. On the other hand, people spend

time outside of their homes, including both more and less polluted microenvironments. This will bias our results to both upward and downward.

One option to estimate the impact of these uncertainties is to compare our results with the studies that take these different microenvironments into account. The Loh et al. (2009) used three different models to predict iFs for benzene emitted from traffic in Helsinki, Finland. The mean iFs for personal measurement model, spatial time activity model and simple box model were 39 per million, 10 per million and 7 per million, respectively. The highest iF were predicted with models that took into account benzene concentration in different microenvironments (e.g. home, work, traffic). In present study we estimated exposure only based on outdoor concentration of pollutants. The results from Loh et al. (2009) suggests that the iF estimates for linear sources would have been higher also in Warsaw, if the exposure in different microenvironments, especially in traffic, would have been taken into account.

4. Conclusions

In this study we have predicted concentrations for different air pollutants in Warsaw, Poland, taking into account emission uncertainties. We also estimated emission-to-exposure relationship for these pollutants using intake fraction (iF) method. To our knowledge this is the first such study made in Warsaw and one of only few studies in the world that have considered iF variation between different emissions sources. All our results have highlighted the important role of traffic for the air quality in Warsaw. The emissions of traffic are high, iF for traffic is higher than for other source categories and, consequently, traffic is main source for most of the air pollutants modeled in this study. From the four emission source categories, high point sources were having only minor impact for local air quality. The iF variation between different emissions sources was significant. This indicates that spatially restricted emissions mitigation actions could have major impact for local air quality and, consequently, to population health. Such emission mitigation action would be e.g. congestion changes, that would reduce the emissions from those areas where they have largest impact for population health.

5. Acknowledgements

We would like to thank Mr. Wojciech Trapp from EKOMETRIA, Poland, for providing the emission data for these calculations and Mr. Bartlomiej Solarz-Niesluchowski from Systems Research Institute, Poland, for setting up the database for the results.

The project (NN519316735) was funded by the Ministry of Science and Higher Education, Poland.

6. References

ApSimon, H.M., Warren R.F., Kayin, S., 2002. Addressing uncertainty in environmental modeling: A case study of integrated assessment of strategies to combat long-range transboundary air pollution. Atmospheric Environment 36, 5417–5426.

Bennett, D.H., McKone, T.E., Evans, J.S., Nazaroff, W.W., Margni, M.D., Jolliet, O., Smith, K.R., 2002a. Defining intake fraction. Environmental Science & Technology 36, 206A-211A.

391 Bennett, D.H., Margni, M.D., McKone, T.E., Jolliet, O., 2002b. Intake fraction for multimedia
392 pollutants: A tool for life cycle analysis and comparative risk assessment. Risk Analysis 22, 905-918.

393 European Environment Agency (EEA), 2009. Population density disaggregated with Corine land cover
394 2000. Available at: http://www.eea.europa.eu/data-and-maps/data/population-density-
395 disaggregated-with-corine-land-cover-2000-2

396 Greco, S.L., Wilson, A.M., Hanna, S.R., Levy, J.I., 2007. Factors influencing mobile source particulate
397 matter emissions-to-exposure relationships in the Boston urban area. Environmental Science &
398 Technology 41, 7675-7682.

399 Hanna, S., Chang, J.C., Fernau, M.E., 1998. Monte Carlo estimates of uncertainties predictions by a
400 photochemical grid model (UAM-IV) due to uncertainties in input variables. Atmospheric
401 Environment 32, 3619–3628.

402 Holnicki, P., Nahorski, Z., Tainio M., 2010. Uncertainty in air quality forecasts caused by emission
403 uncertainty. In: HARMO13, Proceedings of the 13th Conference on Harmonization within
404 Atmospheric Dispersion Modelling for Reegulatory Purposes. Paris, France 1-4 June 2010. Boulogne-
405 Billancourt: ARIA Technologies, pp.119–123.

406 Humbert, S., Manneh, R., Shaked, S., Wannaz, C., Horvath, A., Deschenes, L., Jolliet, O., Margni, M.,
407 2009. Assessing regional intake fractions in North America. Science of the Total Environment 407,
408 4812-4820.

409 Lai, A.C.K., Thatcher, T.L., Nazaroff, W.W., 2000. Inhalation transfer factors for air pollution health
410 risk assessment. Journal of Air & Waste Management Association 50, 1688-1699.

411 Loh, M.M., Soares, J., Karppinen, A., Kukkonen, J., Kangas, L., Riikonen, K., Kousa, A., Asikainen, A.,
412 Jantunen, M., 2009. Intake fraction distributions for benzene from vehicles in the Helsinki
413 metropolitan area. Atmospheric Environment 43, 301-310.

414 Moore, G.E., Londergan, R.J., 2001. Sampled Monte Carlo uncertainty analysis for photochemical
415 grid models. Atmospheric Environment 35, 4863–4876.

416 Page, T., Whyatt, J.D., Beven, K.J., Metcalfe, S.E., 2003. Uncertainty in modeled estimates of acid
417 deposition across Wales: a GLUE approach. Atmospheric Environment 38, 2079–2090.

418 Park, S.K., Cobb, C.E., Wade, K., Mulholland, J., Hu, Y., Russel, A.G., 2006. Uncertainty in air quality
419 model evaluation for particulate matter due to spatial variations in pollutant concentrations.
420 Atmospheric Environment 40, S563–S573.

421 Spadaro, J.V., and Rabl, A., 2004. Pathway analysis for population-total health impacts of toxic metal
422 emissions. Risk Analysis 24, 1121-1141.

423 Russel, A. and Dennis, D., 2000. NASTRO critical review of photochemical models and modeling.
424 Atmospheric Environment 34, 2283–2324.

425 Sax, T,. and Isakov, V., 2003. A case study for assessing uncertainty in local-scale regulatory air
426 quality modeling applications. Atmospheric Environment 37, 3481–3489.

427 Sportisse, B., 2007. A review of current issues in air pollution modeling and simulation.
428 Computational Geosciences 11, 159–181.

429 Taimisto, P., Tainio, M., Karvosenoja, N., Kupiainen, K., Porvari, P., Karppinen, A., Kangas, L.,
430 Kukkonen, J., Tuomisto, J.T., 2011. Evaluation of intake fractions for different subpopulations due to
431 primary fine particulate matter (PM2.5) emitted from domestic wood combustion and traffic in
432 Finland. Air Quality, Atmosphere & Health 4, 199–209.

433 Tainio, M., Sofiev, M., Hujo, M., Tuomisto, J.T., Loh, M., Jantunen, M.J., Karppinen, A., Kangas, L.,
434 Karvosenoja, N., Kupiainen, K., Porvari, P., Kukkonen, J., 2009. Evaluation of the European population
435 intake fractions for European and Finnish anthropogenic primary fine particulate matter emissions.
436 Atmospheric Environment 43, 3052-3059.

437 Wang, S.X., Hao, J.M., Ho, M.S., Li, J., Lu, Y.Q., 2006. Intake fractions of industrial air pollutants in
438 China: Estimation and application. Science of the Total Environment 354, 127-141.

7. Figure captions

Figure 1: Study area, location of the receptor points and the location of the monitoring stations.

Figure 2: Predicted vs. measured annual averaged PM10 concentrations (µg/m3) in 2005.

Figure 3: Average concentration and exposure estimates for different air pollutants. The unit varies between the pollutants. The mean and 95% confidence interval are shown. For some air pollutants, the uncertainty range was too small to be drawn. For acronyms see Table 1.

Figure 4: Uncertainty range and emission sources share for a) particulate matter (PM10) concentrations, b) and PM_S concentration , and c) PM_N concentration for the receptor 275.

Figure 5: Intake fraction (iF) variation between different PPM2.5 emission sources. Largest iFs are predicted for linear and area sources.

8. Tables

Table 1: Air pollutants considered in the present study. Primary pollutants were inputs to the dispersion model. The secondary pollutants were the outputs of the dispersion model, and the concentrations for these pollutants were measured in receptor locations. For SO2 and NOx the emissions and concentrations have different chemical composition, and this difference was taken into account when calculating the iFs.

Primary pollution (emissions)	**Secondary pollution (concentrations)**
PPM2.5 (primary particulate matter (PPM) with aerodynamic diameter ≤ 2.5 μm)	PPM2.5 (PM2.5 concentration caused by the PPM2.5 emissions)
PPM2.5_R (PPM2.5 raised by road traffic – secondary emission)	PPM2.5_R
SO_2 (sulfur dioxide)	PM_S (sulfate ($SO_4^{=}$) aerosol)
NOx (nitrogen oxides)	PM_N (nitrate (NO_3^-) aerosol)
-	PM2.5 = PPM2.5+PPM2.5_R+ PM_S+PM_ H
PPM10 (primary particulate matter with aerodynamic diameter ≤ 10 μm)	PPM10
PPM10_R (PPM10 raised by road traffic – secondary emission)	PPM10_R
-	PM10 = PPM10+PPM10_R+ PM_S+PM_ H
BaP (Benso [a] Pyren)	BaP
Ni (nickel)	Ni
Cd (cadmium)	Cd
Pb (lead)	Pb

458 **Table 2:** Emission volumes and uncertainties (95% confidence interval in brackets). Normal
459 distribution was assumed.

	Unit	Linear sources	Area sources	High point sources	Other point sources
Number of sources	#	1156	877	16	1017
PPM2.5	g/s	15.97 (± 40%)	84.29 (± 40%)	7.61 (± 25%)	15.06 (± 30%)
PPM2.5_R	g/s	26.09 (± 40%)	-	-	-
PM_S	g/s	15.53 (± 30%)	45.77 (± 30%)	885.9 (± 15%)	83.15 (± 20%)
PM_N	g/s	157.2 (± 40%)	22.09 (± 40%)	191.5 (± 20%)	28.81 (± 30%)
PPM10	g/s	24.15 (± 40%)	157 (± 40%)	20.77 (± 25%)	54.19 (± 30%)
PPM10_R	g/s	151.4 (± 40%)	-	-	-
BaP	g/s	0.04 (± 50%)	0.02 (± 50%)	-	0.01 (± 40%)
Cd	µg/s	0.2 (± 50%)	0.02 (± 50%)	-	0.01 (± 40%)
Ni	µg/s	1.96 (± 50%)	0.06 (± 50%)	-	-
Pb	µg/s	106 (± 50%)	0.11 (± 50%)	-	-

460

461

462 **Table 3**: Intake fractions (iF) for different pollutants and source categories. Both mean and variation
463 are shown. Variation represents the minimum and maximum iF calculated for individual sources
464 inside the study area. For example, for PPM2.5 due to linear sources, the minimum calculated iF for
465 any single source area was 1.5 per million. For acronyms see Table 1.
466

Pollutant	Linear sources	Area sources	High point sources	Other point sources	All sources
PPM25	38 (1.5-100)	9.8 (1.6-63)	0.81 (0.050-3.1)	6.6 (0.52-67)	13
PPM25_R	47 (1.6-114)	-	-	-	47
PM_5	0.34 (0.018-0.75)	0.12 (0.029-0.44)	0.013 (0.00080-0.041)	0.066 (0.013-0.44)	0.027
PM_N	0.78 (0.083-1.6)	0.45 (0.17-0.91)	0.029 (0.0017-0.11)	0.21 (0.045-1.6)	0.36
PPM10	38 (1.5-102)	10 (1.6-64)	0.71 (0.051-3.1)	6.2 (0.53-68)	11
PPM10_R	46 (1.6-115)	-	-	-	46
BaP	5.6 (1.3-25)	9.7 (1.6-64)	1.2 (0.31-1.5)	3.3 (1.6-12)	6.0
Cd	5.7 (1.5-25)	11 (1.6-64)	1.2 (0.31-1.5)	3.3 (1.6-12)	5.9
Ni	5.7 (1.5-25)	11 (1.6-64)	-	-	5.9
Pb	40 (1.5-102)	11 (1.6-64)	-	-	40

467

468

469 **Figures**

470 Figure 1

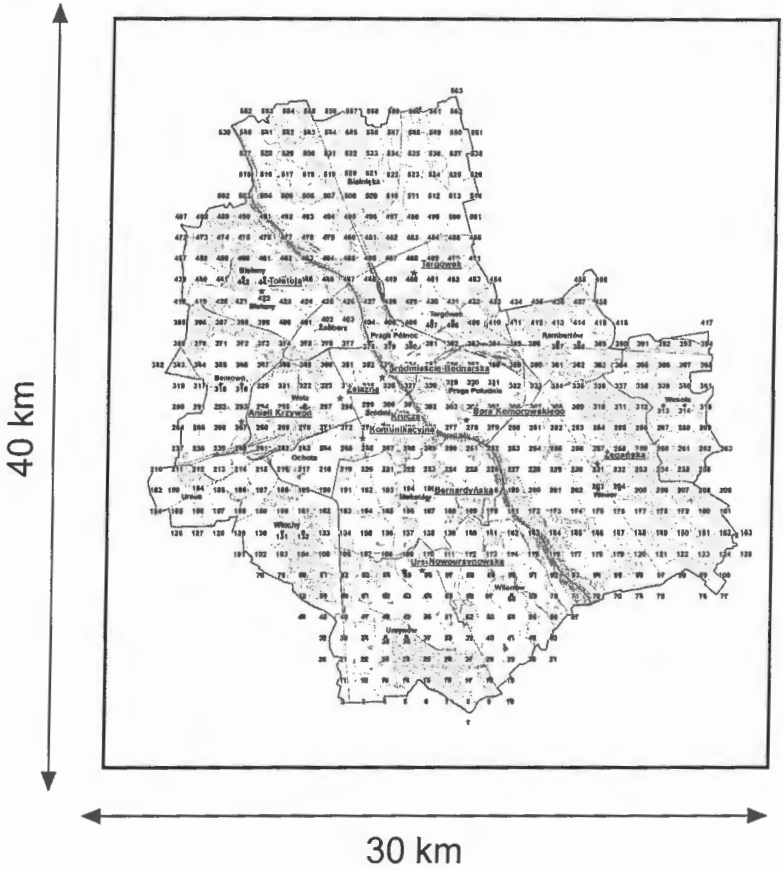

471

472

473

474 Figure 2

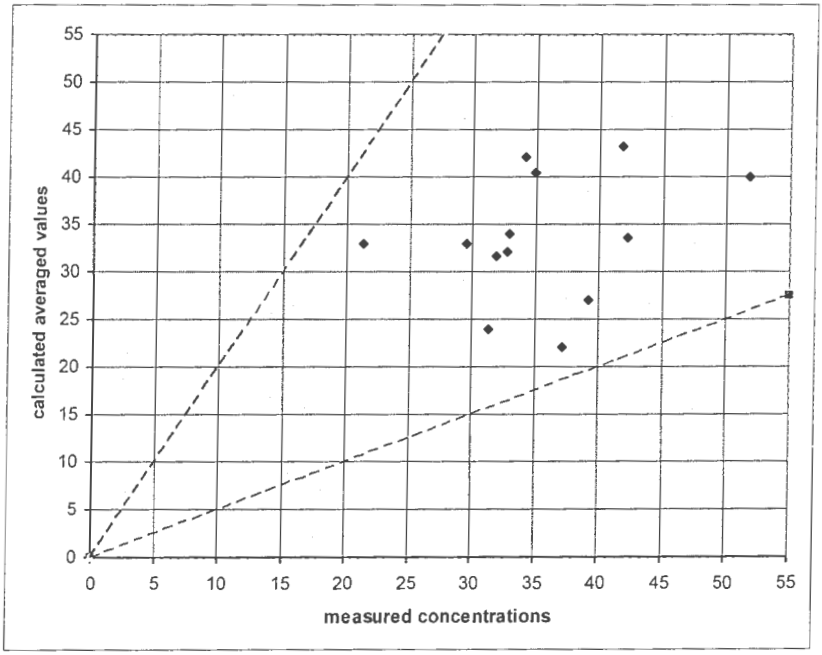

475
476

477

478

479 Figure 3:

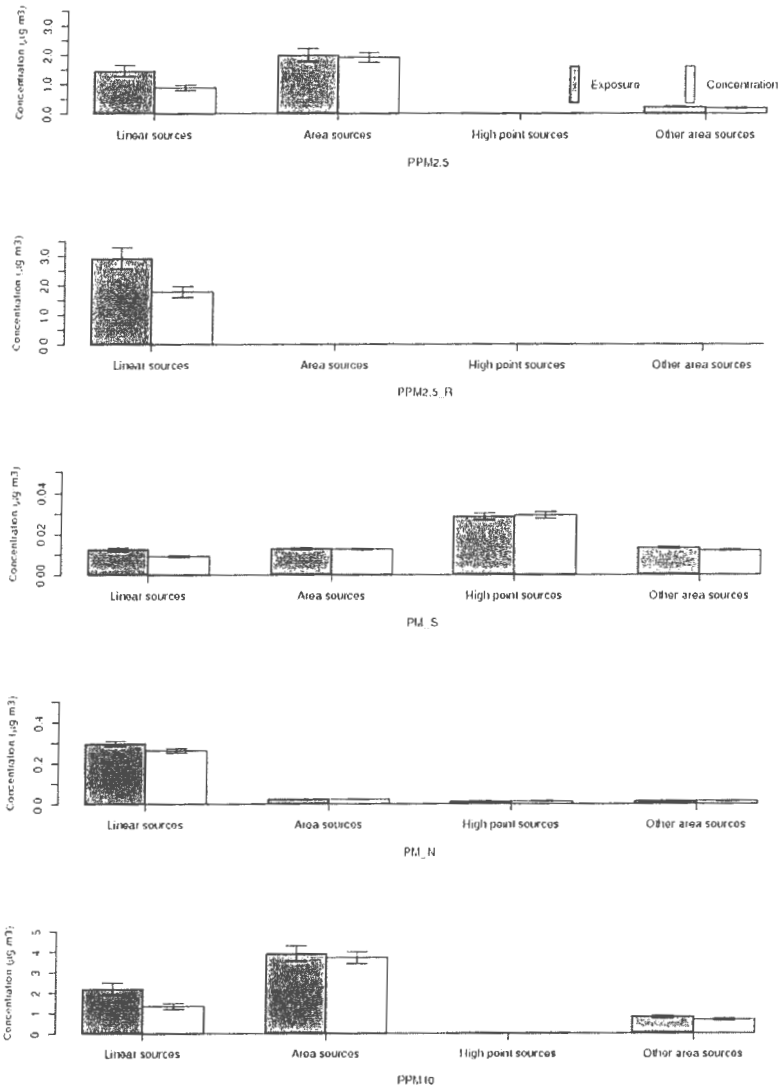

480

481

482 Figure 3 (continues):

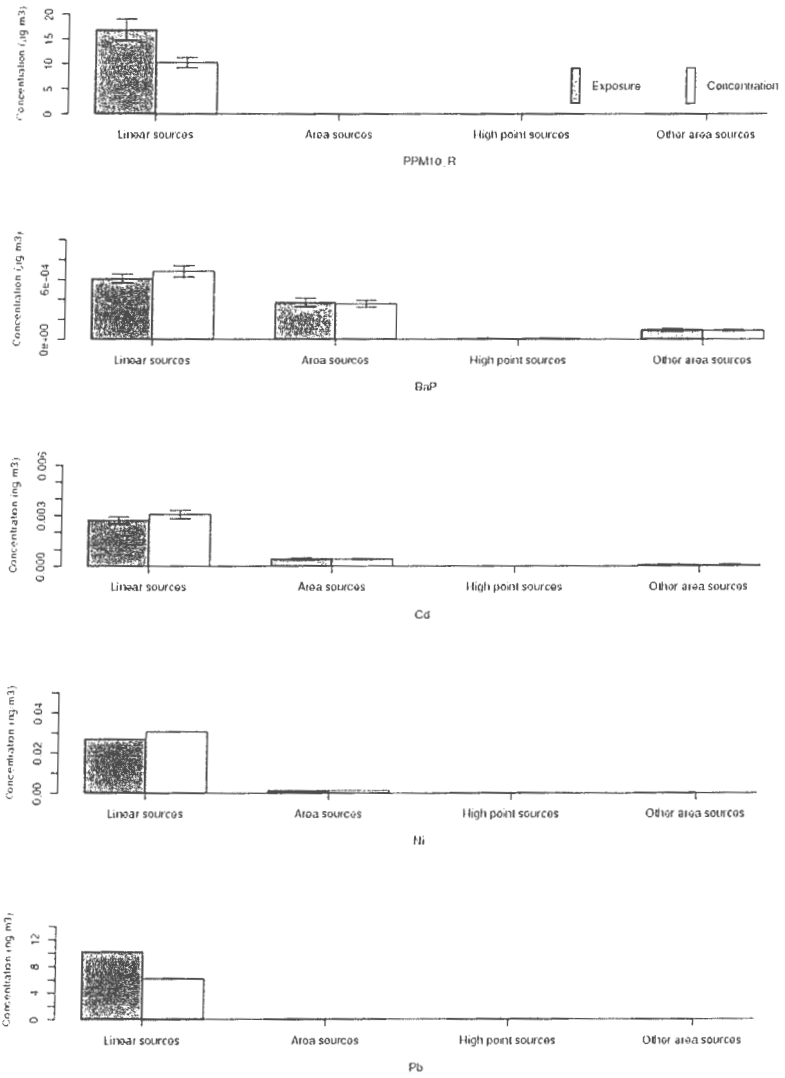

483
484

485 Figure 4
486

a)

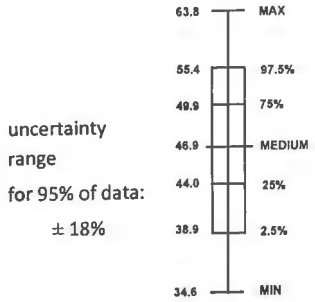

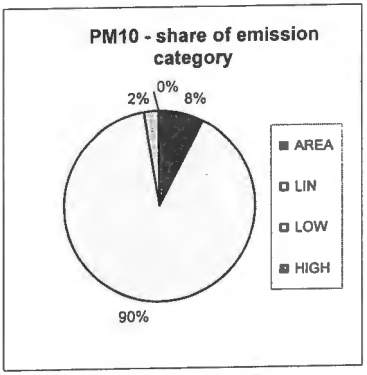

b)

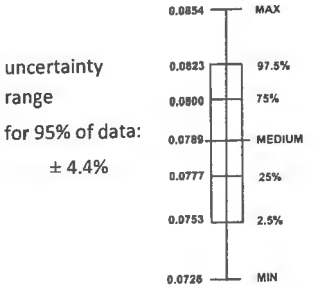

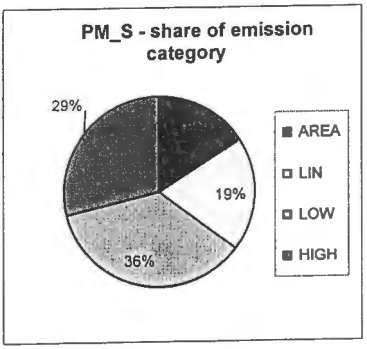

c)

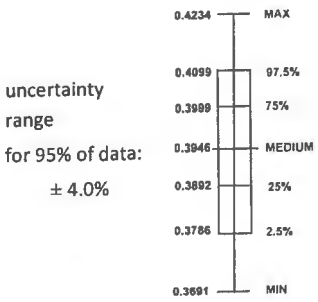

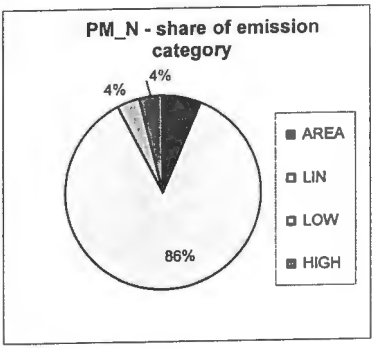

487

488 Figure 5

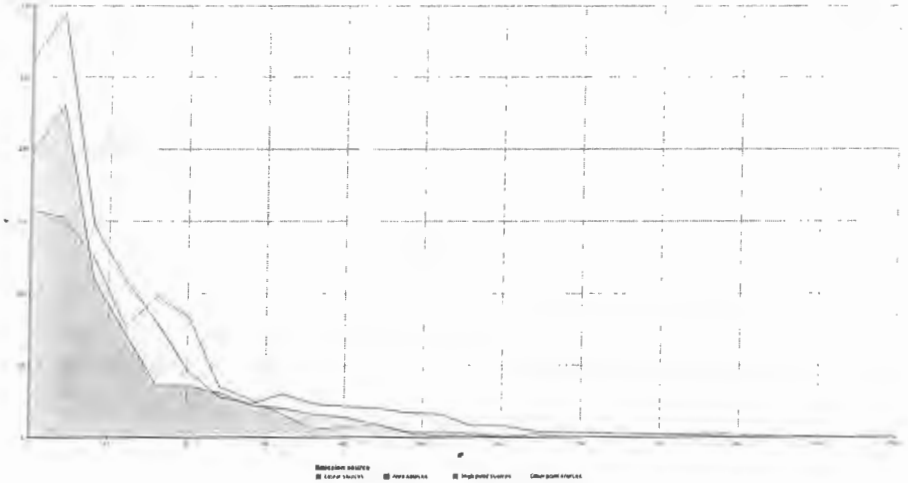

489